The coil–globule transition for a polymer chain confined in a tube: A Monte Carlo simulation

P. Sotta[a)]
Laboratoire de Physique des Solides (CNRS UMR8502), Université Paris-Sud, Bât. 510, 91405 Orsay Cedex, France

A. Lesne and J. M. Victor
Laboratoire de Physique Théorique des Liquides, Université Pierre et Marie Curie, 4, place Jussieu, 75252 Paris Cedex 05, France

(Received 2 June 2000; accepted 27 July 2000)

The behavior of a grafted polymer chain confined in a tube is investigated within a scaling theory substantiated with biased Monte Carlo simulations of a self-avoiding walk (SAW) on a cubic lattice. All the statistical and thermodynamic properties of the chain follow from the knowledge of the joint distribution $P(z,m)$ giving the probability to observe a length z *and* a number of contacts m, in a model where the energy of the chain in a given configuration is proportional to m. The analysis is based on the factorization of $P(z,m)$ into the *a priori* distribution $P(z)$ and the *conditional* probability $P(m|z)$ of finding m contacts *given that* the chain length is z. $P(m|z)$ is well-approximated by a Gaussian distribution. Taking the variance $\langle m^2\rangle - \overline{m^2}$ of this distribution into account, we obtain a nonmean-field expression for the free energy of the confined chain. We show that the coil–globule transition of the confined chain is independent of its size but depends on the pore diameter. Contrary to free, unconfined chains, it is always a continuous transition. © *2000 American Institute of Physics.* [S0021-9606(00)50540-6]

I. INTRODUCTION

The coil–globule transition has been studied theoretically for quite a long time in a free interacting self-avoiding walk (SAW), using various approaches based either on a Flory's argument[1–5] or on more complex methods.[6,7] A phenomenological approach based on numerical simulations was developed.[8–10] On the other hand, the problem of squeezing polymer chains in a pore, either in solution or in melt, is important and has been studied quite extensively.[11–15] The structure of a semidilute solution confined in a porous medium has been studied experimentally, using small angle neutron scattering.[16] In a previous article,[17] we have studied the configurational statistics of a grafted polymer confined in a tube by Monte Carlo simulations. Our numerical model is a SAW on a cubic lattice; successive monomers occupy neighboring sites and the occupancy of neighboring sites by nonconsecutive monomers is called a contact. Within a pair-interaction model, the (Flory) energy of the chain is directly related to the number of contacts. The parameters of the system are the chain length N and the pore diameter D. We have sampled the probability distribution $P(z)$ for the length of tube z occupied by the chain and proposed a scaling expression for this distribution. We also proposed a scaling expression for the average number of contacts in the chain given the length z it occupies in the pore, $m(z)$. A model numerical expression for the free energy of the confined chain as a function of the Flory parameter χ was deduced. It is valid only in the limit of small χ values and amounts to a mean-field approximation. Here, we want to give a more general scaling expression for the free energy of the confined chain, in order to study in more details the polymer behavior in this one-dimensional confined geometry.

The coil–globule transition here is qualitatively different from that of a free, nonconfined polymer. The chain structure in a pore of diameter D is expected to be a linear succession of independent blobs of size D. The transition occurs almost independently within each blob. What happens in a blob is not sensitive to the overall size N of the chain, hence, for a given pore diameter D, no finite size effects are expected on the mean $\langle z\rangle$, $\langle m\rangle$, the density inside the chain, etc. This conjecture will be tested in this work. This argument requires that confining effects operate even in the collapsed (globular) state, or in other words that the globule phase fills more than one blob, i.e., that $N>D^3$. Otherwise, a crossover from a three-dimensional (free chain) behavior (in the condensed state) to a one-dimensional (confined) behavior (in the coil and stretched states) is expected.

Some qualitative features of the coil–globule transition for a free chain in $d=3$ are inferred from the Flory expression of the free energy,[12]

$$\beta F \approx \frac{r^2}{Na^2} + \nu a^3 \frac{N^2}{r^3}, \tag{1}$$

in which the first term is the entropy of the chain and the second one is the mean-field expression for excluded-volume interactions (the short-range repulsion which fixes the density in the globular phase is not included). The adimensional

a)Author to whom correspondence should be addressed. Electronic mail: sotta@lps.u-psud.fr

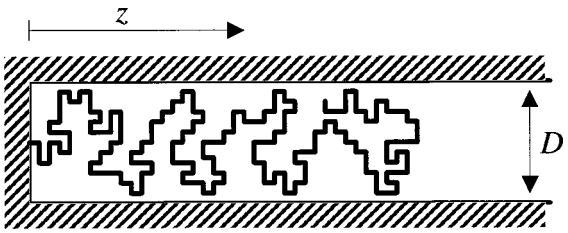

FIG. 1. Schematics of the grafted linear chain confined in a pore, simulated on a cubic lattice.

excluded-volume parameter ν is related to the Flory interaction parameter χ by $\nu=1-2\chi$. Minimizing F gives the equilibrium gyration radius

$$r_F \approx a\,\nu^{1/5} N^{3/5}. \tag{2}$$

The transition towards the Gaussian regime (the so-called θ-solvent, in which $r \approx N^{1/2}$) occurs at $\nu_\theta \approx N^{-1/2}$. This N-dependence describes finite size effects. Note that the Flory expression, Eq. (1), does not describe properly the globule state, but rather the coil and/or stretched states of the chain.[7]

For a polymer confined in a tube of diameter D, the Flory expression now writes[18]

$$\beta F \approx \frac{z^2}{Na^2} + \nu a^3 \frac{N^2}{zD^2}, \tag{3}$$

which gives the equilibrium height of the chain in the pore

$$z_{\mathrm{eq}} \approx a^{5/3} \nu^{1/3} D^{-2/3} N. \tag{4}$$

The scaling prediction, Eq. (4), has been verified in grafted polymer brushes.[19] We set $a=1$ in the following. Introducing the reduced variable $u=zD^{2/3}/N$, the free energy, Eq. (3) may be written

$$\beta F \approx N D^{-4/3} [u^2 + (1-2\chi) u^{-1}]. \tag{5}$$

The N-dependence here is the same in all regimes. Therefore, the coil–globule transition is expected to depend on the pore diameter D but not on N. The aim of the present work is to go a step further than this rough approach and to give a more detailed, nonmean-field description of the coil–globule transition for an isolated chain confined in a pore. It is based on the sampling of the joint probability distribution $P(z,m)$, which gives the probability to obtain a configuration with a height z *and* a number of contacts m.

The article is organized as follows: in Sec. II, we recall scaling arguments and results previously obtained to reconstruct the full distribution (density of states) $P(z,m)$. In Sec. III, we present the results of the numerical simulations. The results are discussed in Sec. IV, an expression for the free energy fitted with numerical results is presented. The features of the coil–globule transition and of some physical properties are discussed.

II. MODEL

Three-dimensional SAW of length N sites are generated on a cubic lattice, using a Monte Carlo method. The chain is confined in a pore and grafted for simulation convenience (see Fig. 1). The pore has a square section of surface area $S=D^2$. The grafting surface and the pore are unpenetrable walls. Elementary moves used to generate chain configurations are free extremity rotations, L-inversions, and kink-shifts.[20,21] There is no bending energy. Different chain lengths ($N=150$ to 500) and different pore sizes ($D=5$ to 11) have been investigated.

The average length of the chain above the grafting surface is defined as

$$z = \frac{1}{N} \sum_{i=1}^{N} z_i, \tag{6}$$

where z_i is the distance of monomer i to the grafting surface. It was shown previously that using z or the gyration radius r_g gives the same results, due to the one-dimensional geometry of this system.[17] The variables sampled during the Monte Carlo simulations are z and m, the total number of contacts between nonconsecutive monomers. The obtained histogram is the joint probability distribution (or density of states) $P_{N,D}(z,m)$, which gives the relative number of configurations with a given length z *and* a given number of contacts m. The modeling of the free energy presented here relies on the following factorization of the joint probability distribution $P_{N,D}(z,m)$:

$$P_{N,D}(z,m) = P_{N,D}(z) P_{N,D}(m|z). \tag{7}$$

The distribution $P_{N,D}(z)$ is the probability to obtain a configuration with a length z and $P(m|z)$ is the *conditional* probability to have a number of contacts m *given that* the length is z.

Note that, in the dense conformations of the chain, there is an important difference between the present case of a polymer confined in a pore of diameter D and a free polymer. In a free polymer, the Edwards' screening length ξ tends to zero (actually, to the monomer size a) when the temperature decreases or in poor solvent, whereas in the pore, it remains comparable to D. One main heuristic assumption here is that the same blob model as in the coil state, remains valid in the globule state.

A. The probability distribution $P(z)$

The distribution $P(z)$ was studied previously.[17] The following scaling form was established:

$$\ln P(z) = -N D^{-5/3} [P_1 u^{-5/4} + P_2 u^{5/2} + P_3 u^5], \tag{8}$$

where u is the reduced variable $u=z/ND^{-2/3}$. Note that the quantity $ND^{-5/3}$ is simply the equilibrium number of blobs in the coil state. P_1, P_2, P_3 are universal coefficients (i.e., independent of N and D) which were determined numerically. The values $P_1 \cong 0.275$, $P_2 \cong 4.03$, and $P_3 \cong 13$ were found. Equation (8) covers a range of u from the condensed state (typically $u_{\min} \cong 0.08$) to the stretched state (typically $u_{\max} \cong 1.5$). No deviation from Eq. (8) at small u values (i.e., higher-order terms) was experienced. However, very small u values, very close to the minimum accessible value, were not sampled. It was shown in Ref. 17 that logarithmic corrections to Eq. (8) are not observed.

B. The average number of contacts $\bar{m}(z)$

The *total* number of contacts in a SAW confined in a pore as a function of the length z was computed previously.[17] A scaling relation was established:

$$m_{D,N}(z)-\langle m_{N,D}\rangle \approx ND^{-5/3}[M_1+M_2u^{-5/4}-M_3u^{5/2}]. \tag{9}$$

M_1, M_2, M_3 are universal coefficients, with numerical values $M_1\cong -1.3$, $M_2\cong 0.54$, and $M_3\cong 3.6$. The M_2-term corresponds to the compact side and the M_3-term to the stretched side. Note that Eq. (9) is valid in the globular regime and in a large interval around the average value $u_m \cong 0.4$. In the stretched regime, $m_{D,N}(z)$ deviates from the above behavior and tends to zero contact.

C. The conditional probability $P(m|z)$

The mean-field approach implemented in Ref. 17 amounts to $P(m|z)\equiv\delta(m-\bar{m}(z))$. In this approximation, the partition function is

$$Z_{N,D}(\chi)=\int\int dz\, dm\, P(z,m)e^{\chi m}=\int dz\, P(z)e^{\chi m}. \tag{10}$$

Here, we use a better approximation, in which the conditional probability $P(m|z)$ is written as a Gaussian distribution

$$P(m|z)=(2\pi\sigma^2)^{-1/2}e^{(m-\bar{m}(z))^2/2\sigma^2(z)}. \tag{11}$$

Then the partition function is

$$Z_{N,D}(\chi)=(2\pi\sigma^2)^{-1/2}\int\int dz\, dm\, P(z)e^{(m-\bar{m}(z))^2/2\sigma^2(z)+\chi m}. \tag{12}$$

In the presence of the $e^{\chi m}$ term, the distribution is centered in $m^*(z)=\bar{m}(z)+\chi\sigma^2(z)$, and integrating over m leads to

$$Z_{N,D}(z,\chi)=P(z)e^{\chi\bar{m}(z)+\chi^2\sigma^2(z)/2}. \tag{13}$$

In the Gaussian approximation, for each z value, the conditional probability is entirely determined by the average $\bar{m}(z)$ and the variance $\sigma^2(z)$, that can be fitted numerically.

The blob picture of the chain in the pore leads to the following scaling properties for $P(m|z)$:

(1) In the ''*stretched state*'' ($z\gg ND^{-2/3}$), the properties of the chain become independent of the pore diameter and the relevant variable is z/N. Thus, as a result of the one-dimensionality of the chain in this regime, one expects $\sigma^2(z)/N$ to be a universal function (i.e., independent of N and D) of the reduced variable z/N.

(2) *In the ''coil'' state* ($z\cong ND^{-2/3}$), the relevant reduced variable is $u=z/ND^{-2/3}$. Still, the chain is a collection of B successive blobs which are statistically independent. This implies that $P_N(m|z)$ is of the form

$$P_N(m|z)\approx\exp\left[-\frac{(m_B-\overline{m_B})^2}{2\sigma_B^2}\right]^B, \tag{14}$$

where m_B is the number of monomers per blob. The variance in one blob is now independent of N. The measured variance $\sigma^2(z)$ is equal to $B\sigma_B^2$, which leads to the scaling relation $\sigma^2(z)/N$ independent of N in this regime as well.

(3) *in the ''condensed'' (globule) state* ($z\approx ND^{-2}\ll ND^{-2/3}$), it was shown in Ref. 9 that the conditional probability may still be written in the form

$$P_N(m|r)\approx[p_t(m/N)]^N, \tag{15}$$

where $p_t(m/N)$ is an effective elementary probability, which accounts for correlations. The variable t, related to the density $\rho=N/zD^2$ (in 3D $t=\rho^{5/4}$), was introduced in Ref. 10 to describe the coil–globule transition. The main difference with a free chain is that the N-dependence is the same in all regimes. Thus, the behavior is not expected to depend on N as it is the case for a free polymer. There are however different dependences on D in the various regimes.

Note that the number of contacts as a function of z (or equivalently u) was computed in Ref. 17 as

$$m_{N,D}(z)=\frac{\Sigma_m mP_{N,D}(z,m)}{\Sigma_m P_{N,D}(z,m)}. \tag{16}$$

Within the Gaussian approximation adopted here, it may alternatively be computed from fitting the conditional probability $P(m|z)$.

III. SIMULATIONS

A. Technicalities

In each simulation, typically 10^7 to 2×10^7 MC steps were performed (one MC step is a cycle of N-attempted elementary moves). The system was equilibrated during a typical time $\tau\cong 0.25N^2$ MC steps before starting the measurements.[22,23]

The distributions $P_{N,D}(z,m)$ are accumulated during the simulations. In order to sample a wide interval of the parameter z, we biased the Monte Carlo simulation with an effective Boltzmann factor (''configurational bias'') of the form e^{Kz} (using a Metropolis algorithm), where K is an adjustable statistical weight. For each K-value, a partial histogram $P_{N,D,K}(z,m)=P_{N,D}(z,m)e^{Kz}$ is obtained, where $P_{N,D}(z,m)$ is the unbiased distribution, sampled in a z-interval which would be impossible to attain in a unbiased simulation. Simulations with positive (negative) values of K sample large (small) values of z. The enlarged distribution $P_{N,D}(z,m)$ is obtained by merging together the histograms $P_{N,D,K}(z,m)$ obtained with different values of K.[9,24,25] (see Appendix). From $P_{N,D}(z,m)$, the distribution $P_{N,D}(z)$ is recovered as

$$P_{N,D}(z)=\sum_m P_{N,D}(z,m).$$

The following procedure may be used as well to get the curves $P(z)$ quickly and accurately. The one-dimensional histogram obtained for a given value K is $h_K(z)=P_{N,D}(z)e^{Kz}$, where $P_{N,D}(z)$ is (a portion of) the unbiased distribution. $h_K(z)$ has its maximum for a value $z_m(K)$ such that $\partial h_K/\partial z=0$, i.e.,

$$\frac{\partial P}{\partial z}+KP=0, \quad \text{or} \quad K=-\frac{\partial \ln P}{\partial z}.$$

TABLE I. The theoretical minimum values $u_{\min}^{\text{th}}$ are obtained by an exact numbering of occupied layers in the tube when the chain is fully compact (i.e., when the density $\rho=1$). $u_{\min}^{\text{scal}}=D^{-4/3}/2$ are the scaling minimum values. Due to the discretization of the lattice, $u_{\min}^{\text{th}}$ values are systematically larger than scaling values $u_{\min}^{\text{scal}}$. $u_{\min}^{\text{exp}}$ are the approximate minimum values effectively sampled. The maximum density values $\rho_{\max}$ are computed as $\rho_{\max}=N/2z_{\min}D^2=1/2u_{\min}^{\text{exp}}D^{4/3}$ obtained from the values effectively obtained $u_{\min}^{\text{exp}}$. ρ_{av} is the average density, i.e., the density obtained in the pore when the chain has its average length.

N	D	$u_{\min}^{\text{th}}$	$u_{\min}^{\text{scal}}$	$u_{\min}^{\text{exp}}$	$\rho_{\max}$	ρ_{av}
150	5	0.0682	0.0585	0.1	0.68	0.2924
200	5	0.0658	0.0585	0.1	0.66	0.2924
200	7	0.0467	0.0373	0.1	0.47	0.1867
300	7	0.0435	0.0373	0.1	0.43	0.1867
400	7	0.0420	0.0373	0.1	0.42	0.1867
400	9	0.0322	0.0267	0.08	0.40	0.1335
500	5	0.0614	0.0585	0.08	0.765	0.2924
500	7	0.041 06	0.0373	0.068	0.6038	0.1867
500	11	0.025 52	0.0204	0.057	0.4477	0.1022

Therefore, plotting K as a function of $u_m(K)$ gives

$$DK(u)=-\frac{\partial}{\partial u}\left[\frac{\ln P}{ND^{-5/3}}\right]. \tag{17}$$

The conditional probability $P_{N,D}(m|z)$ obtained with a statistical weight K does *not* depend on K, only the accessible z-interval does. Thus, in a series of simulations with different statistical weights K, $P_{N,D}(m|z)$ may be obtained directly by fitting the corresponding z-slice of $P_{N,D,K}(z,m)$.

In practice, 8 to 24 different K-values, ranging from -4 to $+4$ typically (and down to -40 in the cases $N=500$), were used in each simulation. Note that another advantage of this procedure is that simulations with different K-values may be run in parallel. In the two-dimensional probability distributions, typically 10^7 independent configurations [i.e., 10^7 values for the couple of parameters (z,m)] are collected. All fits are done by a least-square fit procedure with statistical weighting.

B. Results: The probability distribution $P_{N,D}(u)$

The joint probability distributions $P_{N,D}(z,m)$ have been obtained for different values of the parameters N and D. Then, projection along m gives the distribution

$$P_{N,D}(u)=\sum_m P_{N,D}(u,m),$$

which is expressed here as a function of the reduced variable $u=zD^{2/3}/N$. This distribution was fitted in Ref. 17. The theoretical minimum z and u values which would be obtained in each simulation (corresponding to a completely compact chain) and the minimum values effectively obtained in the simulations, together with the corresponding densities, are summarized in Table I.

The procedure described in Eq. (17) has been used here. According to the scaling Eq. (8),

$$DK(u)=-\frac{\partial}{\partial u}\left[\frac{\ln P}{ND^{-5/3}}\right]$$

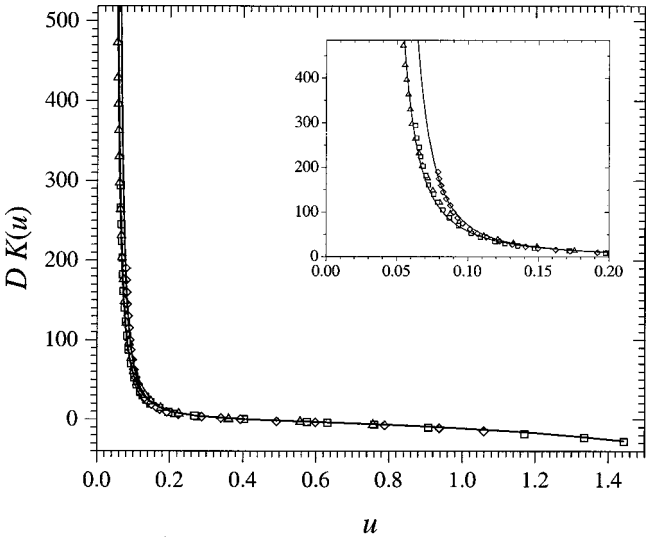

FIG. 2. The curves $DK(u)$ plotted as a function of u, defined as the value corresponding to the maximum of the one-dimensional biased histogram $h_K(z)$. The continuous curves correspond to fits with the function described in Eq. (18). The inset shows an expansion of the small u region. △: $N=500$, $D=11$; □: $N=500$, $D=7$; ◇: $N=500$, $D=5$.

should be a universal function (independent of N and D). In Fig. 2, the curves $DK(u)$ are plotted for several values of the parameters N and D. Excellent superposition on a unique master curve is obtained. Here, the simulations have been extended to u values smaller than in Ref. 17. Deviation from the perfect superposition is observed at very small u values, as it is shown in the inset in Fig. 2. This is due to the finite minimum u value, which differs from one set of parameters to the other. In particular, the discretization of the simulated system starts to play a role in this regime. Higher-order terms have to be introduced at small u values to get satisfactory fits. The curves in Fig. 2 have been fitted with a function of the form

$$\begin{aligned} DK(u)&=-\frac{\partial}{\partial u}\left[\frac{\ln P(u)}{ND^{-5/3}}\right] \\ &=\tfrac{5}{4}P_1u^{-9/4}+\tfrac{5}{2}P_2u^{3/2} \\ &\quad +5P_3D^{-5/3}u^4+(\alpha+1)P_4u^{-\alpha}. \end{aligned} \tag{18}$$

Fitting curves are shown in Fig. 2. A perfect fit is obtained in the whole u range by adding a term $u^{-\alpha}$ with an effective exponent α of the order 6.72. Numerically, the following model expression is obtained for $P(u)$:

$$\begin{aligned} \ln P(u)/ND^{-5/3}=&-0.25u^{-5/4}-4u^{5/2} \\ &-12.5D^{-5/3}u^5-P_4u^{-5.72}. \end{aligned} \tag{19}$$

The coefficients P_1, P_2, P_3 are fairly independent of N and D, as was checked already in Ref. 17. They are robust to introducing the P_4-term. The coefficient P_4 depends significantly on D for a given N value ($N=500$). P_4 ranges from 1.7×10^{-7} (for $D=11$) to 6.2×10^{-7} (for $D=5$).

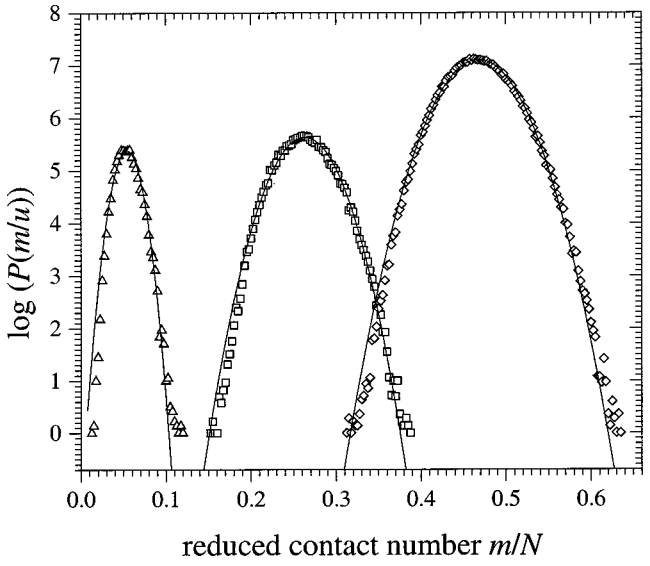

FIG. 3. The logarithm of the conditional probability distribution $\ln P(m|z)$ for different values u corresponding to the stretched, coil, or globule phase of the chain: △: $u=1.5003$; □: $u=0.4025$; ◇: $u=0.1281$. The continuous curves correspond to Gaussian fits of $P(m|z)$, to illustrate the validity of the Gaussian model ($N=400$, $D=7$).

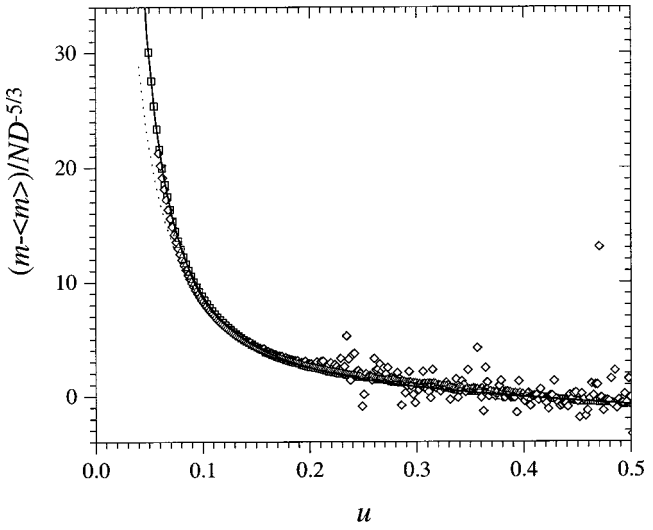

FIG. 4. The reduced number of contacts $(m_{N,D}-\langle m_{N,D}\rangle)/ND^{-5/3}$ as a function of u, for several values of N and D: □: $N=500$, $D=11$; ◇: $N=500$, $D=7$; △: $N=500$, $D=5$; ▽: $N=400$, $D=9$. The continuous curve is the fit of the data $N=500$, $D=11$ with Eq. (20).

C. The conditional probability $P(m|z)$

This is obtained by cutting a slice along m in the 2D distribution $P_{N,D}(z,m)$. $P(m|z)$ is shown in Fig. 3 for different values of the reduced variable $u=z/ND^{-2/3}$ corresponding to the ''coil'' ($u\cong 0.4$) or ''globule'' ($u\cong 0.12$) phase. The stretched case ($u\cong 1.5$) is also illustrated. The corresponding Gaussian fits are also shown in Fig. 3, in order to illustrate the validity of the Gaussian approximation. There is however a systematic, asymmetric deviation from the Gaussian fit, which indicates that higher moments of the distribution (in particular the third one) should be taken into account also. However, this deviation remains small, even in quite compact situations.

D. The average number of contacts

The quantity $(m_{N,D}(u)-\langle m_{N,D}\rangle)/ND^{-5/3}$ is plotted as a function of u in Fig. 4, in a range of u values which corresponds to the coil and compact regimes, for different values of N and D. $m_{N,D}(u)$ was determined from the Gaussian fit of the conditional probability $P(m|z)$. All curves superpose quite exactly, even at very small u values, in accordance to the results in Ref. 17. A higher-order term may be introduced in this regime to improve the fit further. The following numerical model expression gives an excellent fit in the whole sampled u-range:

$$(m_{N,D}(u)-\langle m_{N,D}\rangle)/ND^{-5/3} = 0.54u^{-5/4}-3.62u^{5/2}+0.00647u^{-5/2}. \quad (20)$$

The constant term [M_1 term in Eq. (9)] represents only a slight vertical shift of the curves in the fitted interval, which is negligible here. The coefficient in the $u^{-5/2}$ term depends on D. This is due to the fact that $m_{N,D}(u)$ tends to the maximum number of contacts $2N$ (ignoring surface terms) when u tends to the minimum value $u_{\min}\approx D^{-4/3}/2$. The conjectures leading to the scaling expressions in Eqs. (8) and (9) were essentially based on the blob picture for the confined chain. More precisely, the portion of chain inside a blob should behave as a free chain, as regards its statistical behavior. Thus, it may be checked that the numerical result in Eq. (20) is in concordance with the number of contacts $m_N(R)$ in a free polymer of the same size and density as the considered blob. In Ref. 6, it was shown that $m_N(R)$ may be written $m_N(R)=aN+Bs^{-15/4}-Cs^{-5/2}-Ds^{5/2}+E$, s being the reduced gyration radius $s=R/R_0$ with R_0 the equilibrium gyration radius of a SAW in good solvent. The C-term is the surface term, the B-term describes the compact side ($s\ll 1$), and the D-term the coil region ($s\geqslant 1$). $m_N(R)$ may be rewritten in terms of the density defined as $\rho=N/R^3=N/R_0^3s^3$ (given that $R_0\cong\lambda_0N^{3/5}$ with $\lambda_0=0.396$):[25] $m_N(\rho)\approx N\rho^{5/4}-N^{-2/3}\rho^{-5/6}$ (only B and D terms have been written). Then, to compare to the case of a polymer in a pore, N in the formula above should first be set equal to the number of monomers in one blob $g=\rho D^3$, then the number of contacts in one blob should be multiplied by the number of blobs $B=N/g$. Finally, given the numerical values in Ref. 6, the blob picture leads to

$$m_{N,D}(\rho)\approx 0.15N\rho^{5/4}-14.2ND^{-5}\rho^{-5/2}. \quad (21)$$

Numerically, it was found in Ref. 17 (only the B and D terms are indicated) $m_{N,D}(r/r_0)\approx ND^{-5/3}\lfloor 1.65(r/r_0)^{-5/4}-0.35(r/r_0)^{5/2}\rfloor$, which may be rewritten, given that $r_0=\lambda_1ND^{-2/3}$ (with $\lambda_1=0.22$) and $r=N/\rho D^2$ as

$$m_{N,D}(\rho)\approx 0.25N\rho^{5/4}-15.4ND^{-5}\rho^{-5/2}. \quad (22)$$

The numerical coefficients in Eqs. (21) and (22) are indeed quite close, even though geometrical details in the confined chain have been largely ignored. Thus, the comparison between Eqs. (21) and (22) strongly supports the blob model for the confined chain.

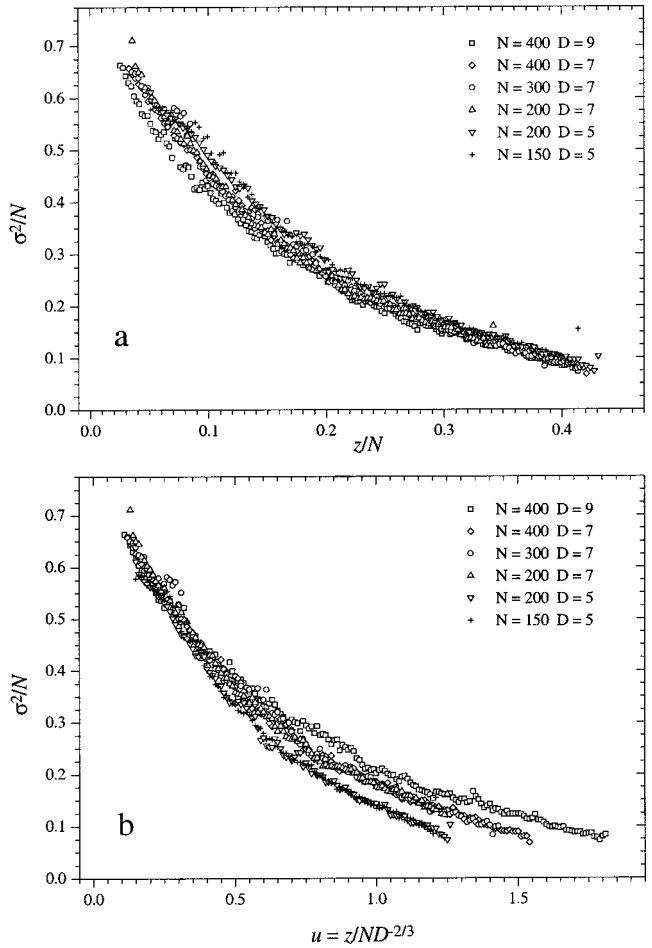

FIG. 5. (a) The quantity $\sigma^2(z)/N$ plotted as a function of z/N, for different values of N and D. $\sigma^2(z)$ is obtained by a least-square fit of the conditional probability $P(m|z)$ with a Gaussian function. (b) $\sigma^2(z)/N$ plotted as a function of u.

E. Fit of the variance $\sigma^2(z)$

As the average number of contacts $\overline{m}$, the variance $\sigma^2(z)$ may be computed in two different ways, either from the Gaussian fit of $P(m|z)$, or directly as

$$\sigma^2 = \frac{\Sigma_i m_i^2 P(m_i)}{\Sigma_i P(m_i)} - \overline{m}^2. \tag{23}$$

We have checked that both measurements coincide within error bars. The second moment taken from the Gaussian fit, that includes in an effective way higher-order statistical deviations, coincides with the actual variance, which justifies the Gaussian approximation adopted here. The variance $\sigma^2(z)$ shown in the forthcoming figures has been obtained from the Gaussian fit of $P(m|z)$.

The different regimes mentioned in Sec. II B may be distinguished as follows. According to the scaling laws related to the one-dimensional character of the chain, the quantity $\sigma^2(z)/N$ should be independent of N. In Fig. 5(a), the quantity $\sigma^2(z)/N$ is plotted as a function of the variable z/N, for different values of N and D. The curves tend to collapse on a single master curve at large z-values, and show a relatively good superposition property over a large range of z-values. This corresponds to the scaling quoted in Sec. II B

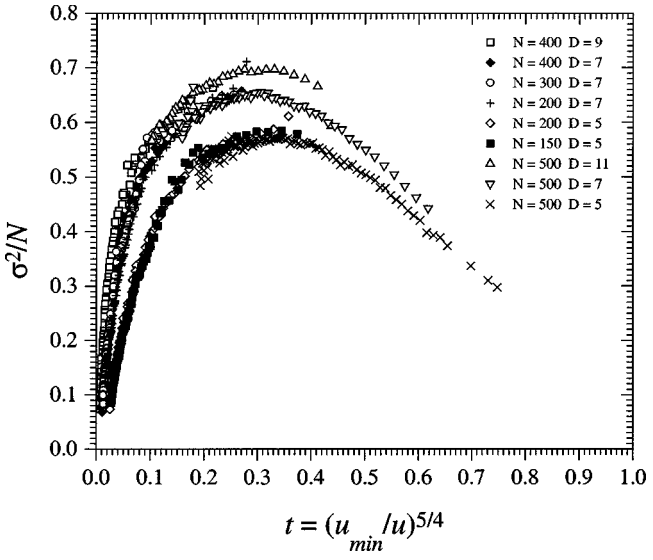

FIG. 6. The quantity $\sigma^2(z)/N$ plotted as a function of $t=(u_{\min}/u)^{5/4}$, for different values of N and D.

in the *stretched regime*, i.e., for large z-values. In the *coil regime*, the relevant variable is u. In Fig. 5(b), the curves $\sigma^2(z)/N$ are plotted as a function of u. Indeed, the curves superpose relatively well in the coil regime, i.e., around $u=0.4$. In the *globule* ($u<0.4$) regime, the relevant variable is the density $\rho=u_{\min}/u$, or equivalently the variable related to it $t=\rho^{5/4}$. $u_{\min}$ is the minimum value of u that would correspond to a fully compact chain ($\rho=1$). In Fig. 6, the curves $\sigma^2(z)/N$ are plotted as a function of t. The value $u_{\min}$ used to define the variable t in Fig. 6 is the actual value, denoted $u_{\min}^{\text{th}}$ in Table I. The maximum density is then $\rho_{max}=1$ in the plot in Fig. 6.

It is observed in Fig. 6 that the curves corresponding to one given value of D and various N-values (from 150 to 500) collapse on a single curve. There is however a significant variation on D: the curves obtained for different D values have the same general behavior but do not superpose.

For a given value of D, the quantity σ^2/N is proportional to the variance in one blob, which depends on D only. Then, it is expected that the larger the blob size D, the larger the variance, which is indeed observed in Fig. 6. Thus, the increasing D-variation observed in Fig. 6 is consistent with the blob picture.

The quantity σ^2/N is the variance of the function $p_t(m/N)$ as defined in Eq. (15). The variance of $p_t(m/N)$ was measured for free, unconfined chains in Ref. 9. The curves in Fig. 6 reflect a behavior within one blob qualitatively similar to that observed in free chains. The numerical values are however higher in the present case. In Ref. 9, the curves were fitted to a function of the form $\sigma^2(t)=\sigma_0^2+\sigma_1^2 t+\sigma_2^2 t^\alpha \ln t$ with α of the order 0.5 in three dimensions. In Fig. 7, the curves σ^2/N corresponding to $D=7$ and various values of N are plotted as a function of t. The curves can be satisfactorily fitted by a function of the form $f(t)=\Sigma^2 t^\alpha \ln t$. There is however a significant difference with respect to free chains: the density (or equivalently the variable t) as it is defined here does not tend to zero in the stretched regime in the limit $N\to\infty$, but to a value $t_{\min}$

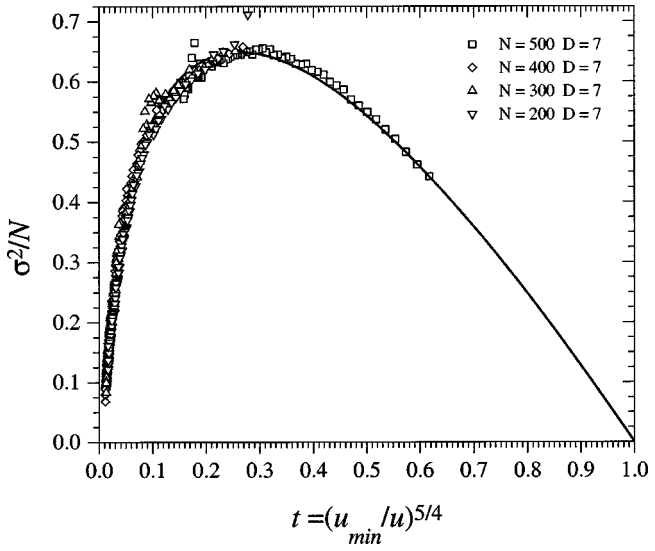

FIG. 7. The quantity $\sigma^2(z)/N$ plotted as a function of $t=(u_{\min}/u)^{5/4}$, for $D=7$ and different values of N. The continuous curve is a fit using Eq. (24).

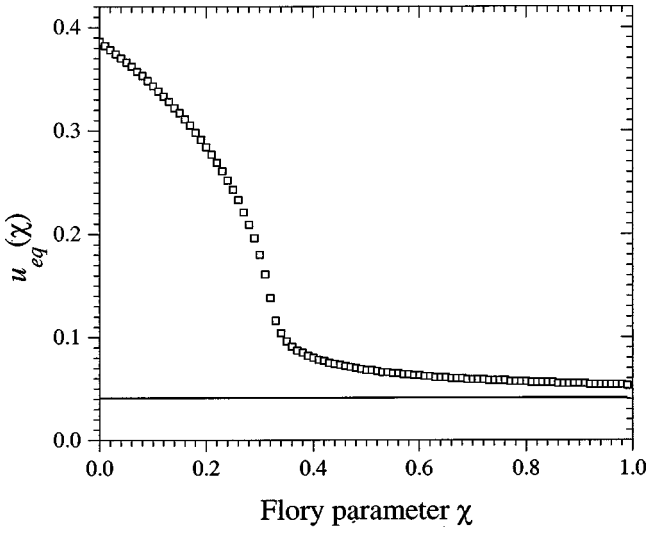

FIG. 8. The curve $u_{\mathrm{eq}}(\chi)$ obtained by minimizing the free energy, Eq. (25), for $N=500$ and $D=7$.

$=D^{-5/2}$ (which depends on D only). To take this behavior into account, we have fitted the curves $\sigma^2(t)/N$ with a function of the form

$$f(t)=\Sigma^2 t'^{\alpha}\ln t' \quad \text{with} \quad t'=\frac{t-t_{\min}}{1-t_{\min}}. \tag{24}$$

This modification $t\to t'$ has no effect on the fit in the compact regime (i.e., for t close to one). Good fits are obtained in the whole range of the variable t', as is shown in Fig. 7. The adjustable parameters Σ^2 and α are summarized in Table II for $N=500$ and various D-values. Note that Eq. (24) is a purely phenomenological function. There is no theoretical account for it at the moment.

IV. IS THERE A COIL–GLOBULE TRANSITION?

A. Free energy of the confined chain

A numerical model expression may now be proposed for the free energy of a SAW confined in a pore, within the Gaussian approximation. In this model, each contact is supposed to reduce the energy by an amount $k_BT\chi$, where χ is the Flory interaction parameter. The free energy, considered as a function of z (or equivalently u) and χ, is defined as $F_{N,D}(z,\chi)=-k_BT\ln Z_{N,D}(z,\chi)$, where $Z_{N,D}(z,\chi)$ is the z-partition function defined in Eq. (13). This gives

$$\frac{F_{N,D}(u,\chi)}{k_BT}=-\ln P_{N,D}(u)-\chi m(u)-\frac{1}{2}\chi^2\sigma^2(u). \tag{25}$$

TABLE II. Fitting parameters obtained when fitting the curves $\sigma^2(t)/N$ with Eq. (24), for $N=500$ and various values of the pore diameter D.

N	D	Σ^2	α
500	5	−1.265	0.814
500	7	−1.307	0.737
500	11	−1.54	0.81

The structure of the free energy, Eq. (25), is similar to the Flory expression. Compared to the mean-field expression,[17] there is an extra factor $\chi^2\sigma^2/2$, which is expected to vanish in the completely compact state of the chain. This term plays a role similar to the three-body term in the Flory free energy.

The equilibrium value $u_{\mathrm{eq}}(\chi)$ is obtained by minimizing $F_{N,D}(u,\chi)$ for each given value of χ. An example of the curves $u_{\mathrm{eq}}(\chi)$ obtained in this way is shown in Fig. 8 for the case $N=500$ and $D=7$. The continuous, horizontal line indicates the value of u which would correspond to the fully collapsed chain ($\rho=1$).

Replacing u by the equilibrium value $u_{\mathrm{eq}}(\chi)$ in Eq. (25), one may obtain the equilibrium free energy as a function of χ, $F_{\mathrm{eq}}(\chi)$, or equivalently as a function of $T(T=1/\chi)$. It is clear from Eq. (25) that the quantity $F_{\mathrm{eq}}(\chi)/N$ is universal, i.e., independent of the chain length N, given the scaling relations, Eqs. (19), (20), and (24). This means that there is no finite-size effect in the present problem. This is in contrast to the case of a *free* polymer chain, in which the equilibrium free energy depends on the chain length N. Given the numerical values of the various terms in Eq. (25), it is found also that the scaled quantity $F_{\mathrm{eq}}(\chi)/ND^{-5/3}$ is independent of D as well, to an excellent approximation.

B. Nature of the coil–globule transition

The main conclusion from this work is that the coil–globule transition for a chain confined in a pore is continuous. This result comes from two specific features. First, the chain confined in a linear pore may be analyzed as a linear succession of statistically independent blobs. The free energy is essentially extensive in the number of blobs. The transition occurs within each blob independently. It results that the overall chain length N is not relevant to discuss finite size effects, but rather the number g of monomers per blob. The relevant quantity to describe the confined chain is then the Boltzmann–Gibbs distribution for one blob $P_g(t,\chi)$ [or equivalently the free energy per blob as it may be defined

from Eq. (25)], expressed here in terms of the Flory parameter χ and the variable t defined in the same way as in Sec. III E. It is shown in Refs. 10 and 26 that for small chains, the coil–globule Θ-point always corresponds to a continuous transition. Whereas for long chains the Boltzmann–Gibbs distribution $P_N(t,\chi)$ is bimodal in some range of χ (or temperature T), giving rise to a first-order transition, it always has only one maximum for small chains, this maximum being shifted continuously towards the globular state as χ increases (or as T decreases).

Another potentially interesting consequence of the blob structure of the chain may be the chain response to stretching. It was shown in Refs. 27, 28 that applying a stretching force to a chain collapsed in a poor solvent (i.e., in the globular state) gives rise to a discontinuous, first order unwinding transition. It is expected in the present case that each blob will unwind independently on stretching the confined chain, which will lead to a continuous unwinding.

V. CONCLUSION

The two-dimensional joint probability distribution $P_{N,D}(z,m)$ for the length z and the number of contacts m of a linear, neutral SAW of length N confined in a tube of diameter D, contains all the relevant statistical information on this system. This quantity has been investigated using biased Monte Carlo simulations. Writing $P_{N,D}(z,m) = P_{N,D}(z)P_{N,D}(m|z)$, we have computed a nonmean-field expression for the free energy of the confined chain, by taking into account the second moment of the conditional probability distribution $P_{N,D}(m|z)$. This may be used to study the coil–globule transition in the confined chain as the temperature or the quality of the solvent is varied. The results presented here strongly reinforce the ''blob'' picture: they indicate that the transition occurs within each blob independently. As a consequence, the transition is always continuous, contrary to the case of a free, unconfined linear chain.

APPENDIX

The overall unbiased distributions $P_{N,D}(z,m)$ is obtained by merging together the biased two-dimensional probability distributions (histograms) sampled numerically.

Suppose that two two-dimensional histograms $h_i(z,m)$ and $h_j(z,m)$ have been generated with two different values of the statistical weight parameter K_i and K_j, respectively. The distributions $H_i(z,m)=h_i(z,m)e^{K_i z}$ and $H_j(z,m) = h_j(z,m)e^{K_j z}$ are portions of the *same*, unbiased distribution (sampled on different z-intervals, however). The different portions $H_i(z,m)$ are normalized and merged using statistical weighting, that is, the relative normalization (translation) factor τ_{ij} is computed by minimizing the quantity

$$Q=\sum_{z,m} \lambda_{ij}(z,m)[\ln H_i(z,m)-\ln H_j(z,m)-\tau_{ij}]^2.$$

The weighting factor $\lambda_{ij}(z,m)$ takes into account the statistical weight in each file, i.e., $\lambda_{ij}(z,m)=[h_i(z,m)^{-1} + h_j(z,m)^{-1}]^{-1}$ [$\lambda_{ij}(z,m)=0$ if one of the files, $h(z,m)$, is zero].

This leads to

$$\tau_{ij}=\frac{\Sigma_{z,m}\lambda_{ij}(z,m)[\ln H_i(z,m)-\ln H_j(z,m)]}{\Sigma_{z,m}\lambda_{ij}(z,m)}.$$

Then, all files are merged together to give the logarithm of the final, reconstructed distribution $H(z,m)$

$$\ln H(z,m)=\frac{\Sigma_i h_i(z,m)[\ln H_i(z,m)-\tau_{i0}]}{\Sigma_i h_i(z,m)}.$$

[1] P. G. de Gennes, J. Phys. (France) Lett. **36**, 55 (1975).
[2] C. B. Post and B. H. Zimm, Biopolymers **18**, 1487 (1979).
[3] I. C. Sanchez, Macromolecules **12**, 980 (1979).
[4] E. A. DiMarzio, J. Chem. Phys. **81**, 969 (1984).
[5] M. Muthukumar, J. Chem. Phys. **81**, 6272 (1984).
[6] I. M. Lifshitz, A. Y. Grosberg, and A. R. Khokhlov, Rev. Mod. Phys. **50**, 683 (1978).
[7] T. M. Birshtein and V. A. Pryamitsyn, Macromolecules **24**, 1554 (1991).
[8] J. M. Victor, J. B. Imbert, and D. Lhuillier, J. Chem. Phys. **100**, 5372 (1994).
[9] J. B. Imbert and J. M. Victor, Mol. Simul. **16**, 399 (1996).
[10] J. B. Imbert, A. Lesne, and J. M. Victor, Phys. Rev. E **56**, 5630 (1997).
[11] M. Daoud and P. G. de Gennes, J. Phys. (France) **38**, 85 (1977).
[12] P. G. de Gennes, *Scaling Concepts in Polymer Physics* (Cornell University Press, Ithaca, New York, 1979).
[13] F. Brochard and P. G. de Gennes, J. Phys. (France) **40**, L-399 (1979).
[14] A. Milchev, W. Paul, and K. Binder, Macromol. Theory Simul. **3**, 305 (1994).
[15] T. W. Burkhardt, Phys. Rev. E **59**, 5833 (1999).
[16] J. Lal, S. K. Sinha, and L. Auvray, J. Phys. II **7**, 1597 (1997).
[17] P. Sotta, A. Lesne, and J. M. Victor, J. Chem. Phys. **112**, 1565 (2000).
[18] D. Lhuillier, J. Phys. (France) Lett. **49**, 705 (1988).
[19] Pik-Yin Lai and K. Binder, J. Chem. Phys. **95**, 9288 (1991).
[20] J. Reiter, T. Edling, and T. Pakula, J. Chem. Phys. **93**, 837 (1990).
[21] J. Reiter, Macromolecules **23**, 3811 (1990).
[22] A. Chakrabarti and R. Toral, Macromolecules **23**, 2016 (1990).
[23] M. T. Gurler, C. C. Crabb, D. M. Dahlin, and J. Kovac, Macromolecules **16**, 398 (1983).
[24] A. M. Ferrenberg and R. H. Swendsen, Phys. Rev. Lett. **61**, 2635 (1988).
[25] J. B. Imbert, Ph.D. thesis, Université Paris VI, 1995.
[26] A. Lesne and J. M. Victor, Phys. Rev. Lett. (submitted).
[27] Pik-Yin Lai, Phys. Rev. E **53**, 3819 (1996).
[28] Pik-Yin Lai, Phys. Rev. E **58**, 6222 (1998).